Electronic Supplementary Material (ESI) for Inorganic Chemistry Frontiers.

Supporting Information

Tailoring Two Magic Number Gold Nanoclusters Au_{13} with N-Containing Diphosphine Ligands: Classical Icosahedral Core *vs.* Unprecedented *UFO*-Shaped Core

Jing Liu, Jia-Chuan Liu, Hai-Ling Wang, Pei-Yu Liao, Jian-Hua Jia* and Ming-Liang Tong

Key Laboratory of Bioinorganic and Synthetic Chemistry of Ministry of Education, School of Chemistry, IGCME, GBRCE for Functional Molecular Engineering, Sun Yat-Sen University, Guangzhou 510006, Guangdong, P. R. China.

Corresponding Author(s): jiajh3@mail.sysu.edu.cn

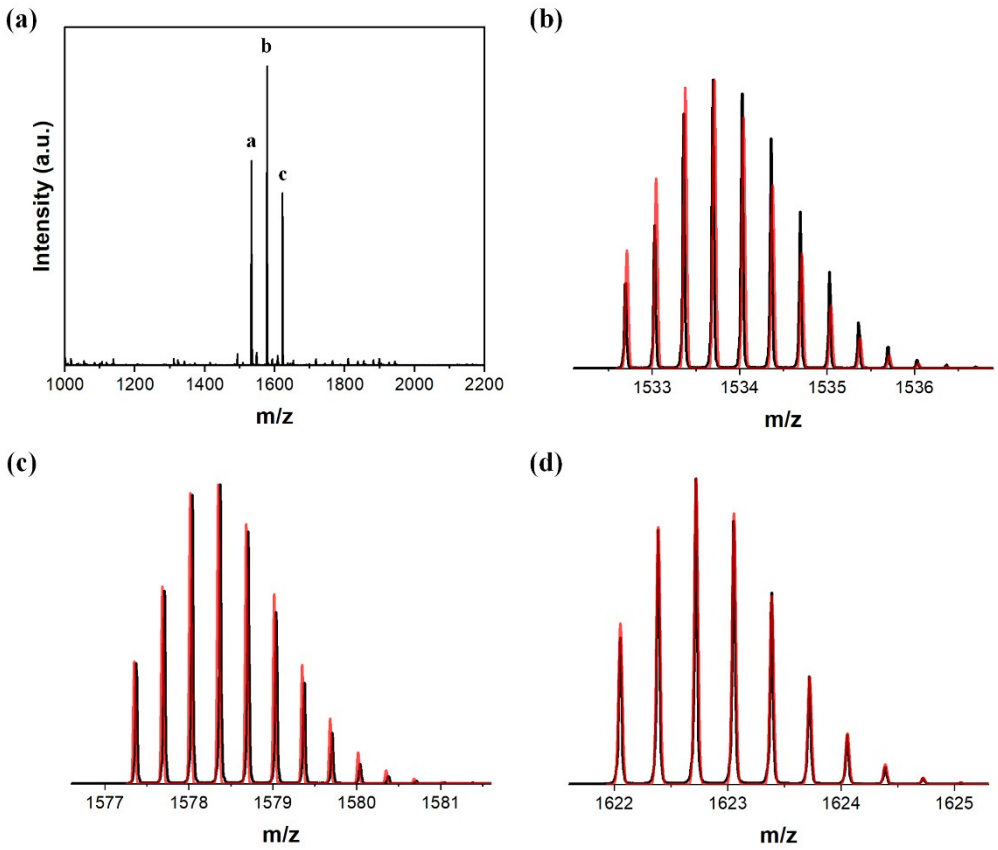

Fig. S1 ESI-MS in positive mode of **1** in DCM (a), and the comparison of experimental (black line) and simulated (red line) isotope patterns of peak a, $[Au_{11}(PNP)_5+KCl+DCM+K^+–H^+]^{3+}$, m/z = 1533.70, calcd. 1533.71 (b); peak b, $[(Au_{11}(PNP)_5+KCl+DCM+K^+–2H^+)+Cs^+]^{3+}$, m/z = 1578.37, calcd. 1578.35 (c); peak c, $[\mathbf{1}]^{3+}$, m/z = 1622.72, calcd. 1622.72 (d).

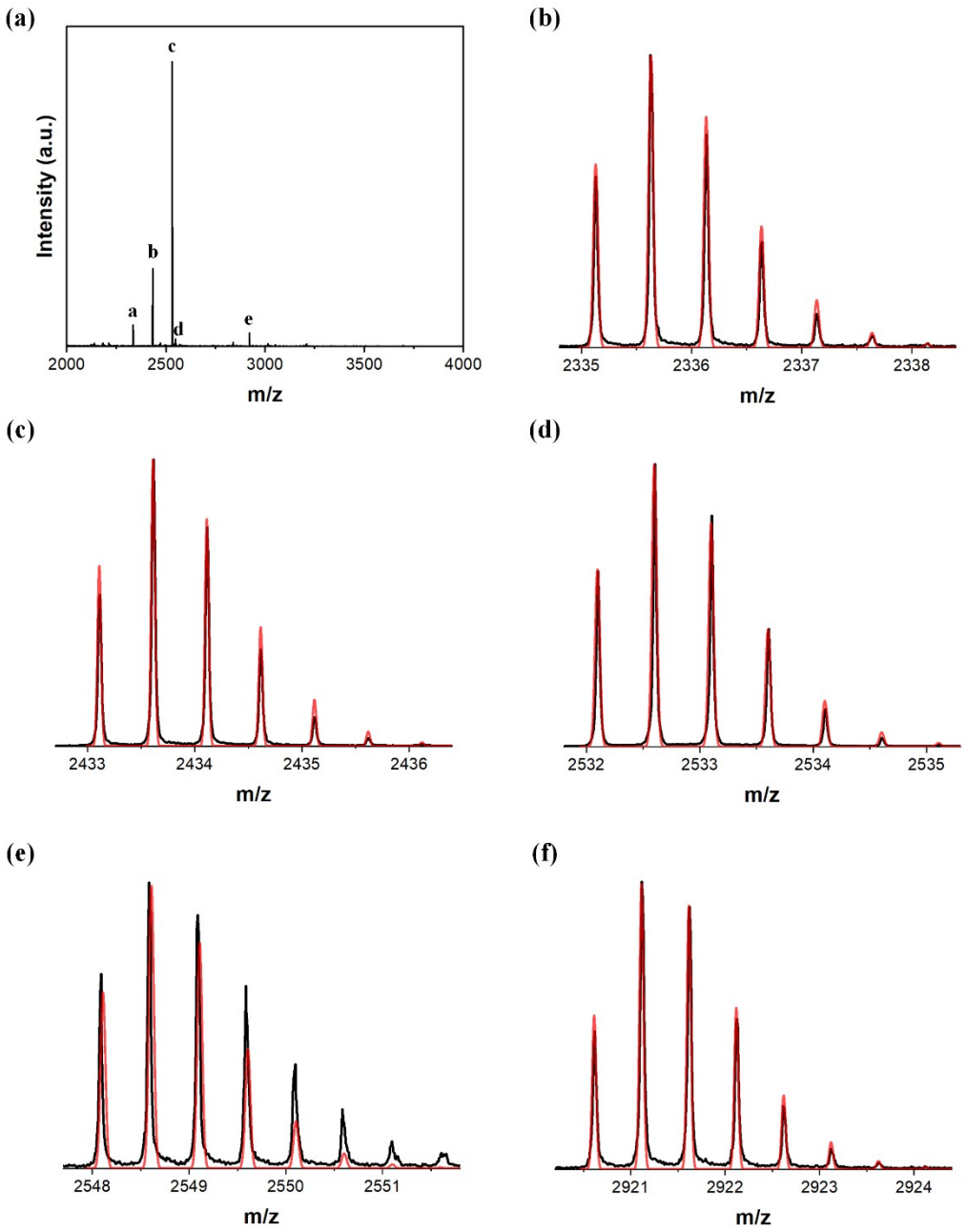

Fig. S2 ESI-MS in positive mode of **2** in DCM (a), and the comparison of experimental (black line) and simulated (red line) isotope patterns of peak a, [$\mathbf{2}^{5+}$–Au^{+}–$2H^{+}$]$^{2+}$, m/z = 2335.63, calcd. 2335.63, (b); peak b, [$\mathbf{2}^{5+}$–$3H^{+}$]$^{2+}$, m/z = 2433.62, calcd. 2433.61, (c); peak c, [$\mathbf{2}^{5+}$–$4H^{+}$+Au^{+}]$^{2+}$, m/z = 2532.60, calcd. 2532.60, (d); peak d, [$\mathbf{2}^{5+}$–$4H^{+}$+Au^{+}+MeOH]$^{2+}$, m/z = 2548.58, calcd. 2548.61, (e); peak e, [$\mathbf{2}^{5+}$–$6H^{+}$+$3Au^{+}$+Hdppa]$^{2+}$, m/z = 2921.12, calcd. 2921.11, (f).

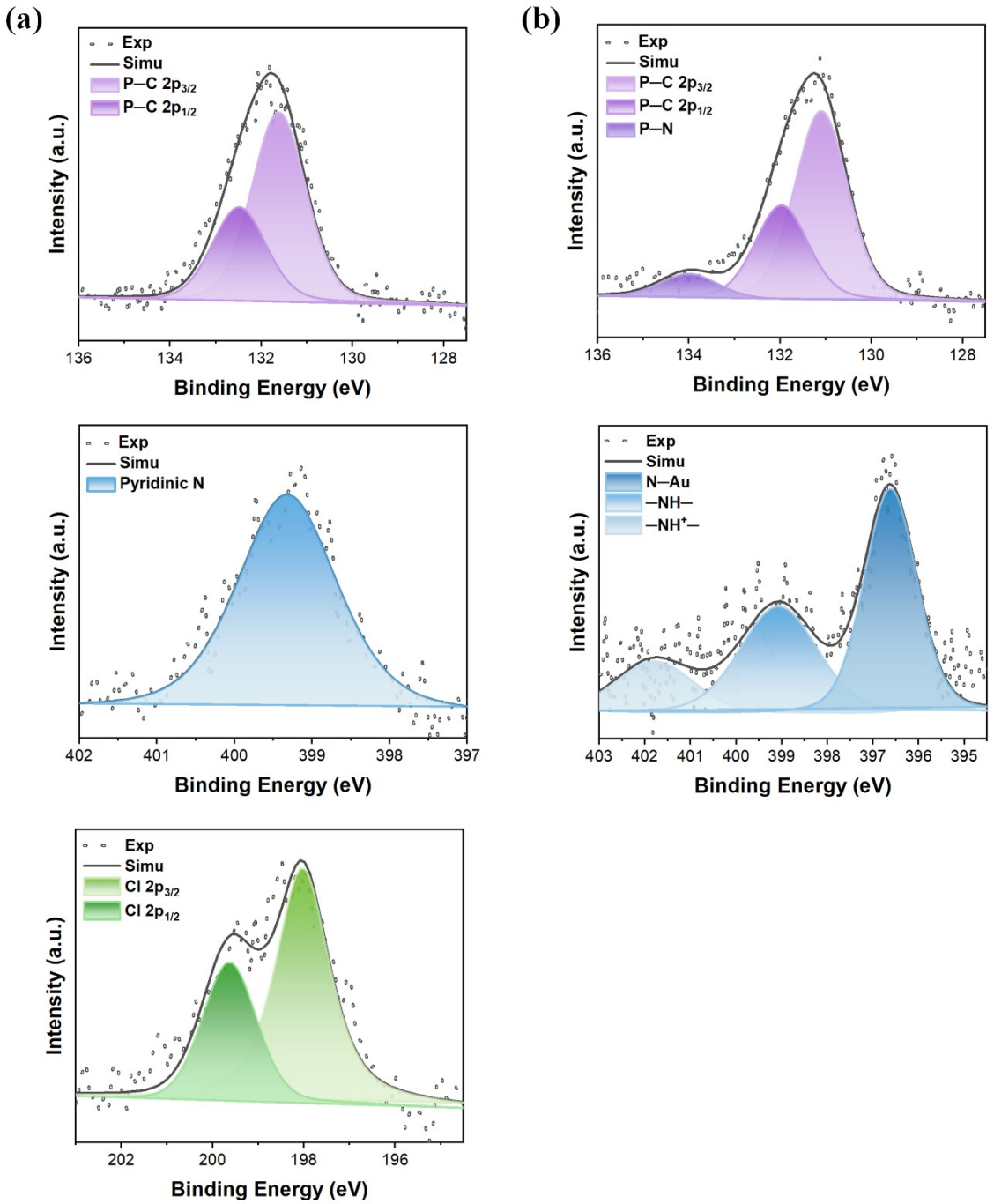

Fig. S3 XPS core level spectra of P 2p (top), N 1s (middle) and Cl 2p (bottom) for **1** (a) and **2** (b).

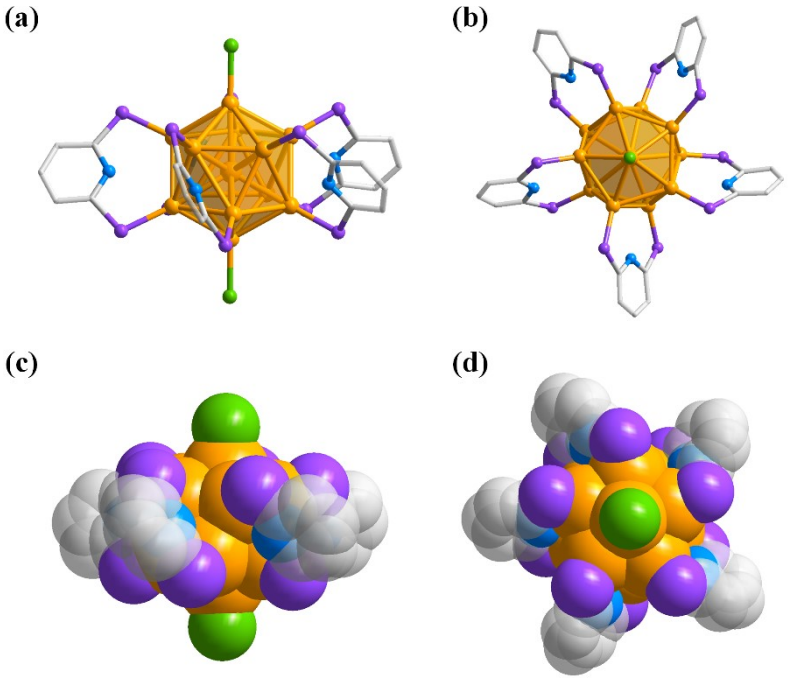

Fig. S4 Molecular structure and space-filling mode of **1**. Color legend: Au, orange; Cl, green; P, purple; N, blue; C, gray. All aromatic rings and hydrogen atoms are omitted for clarity.

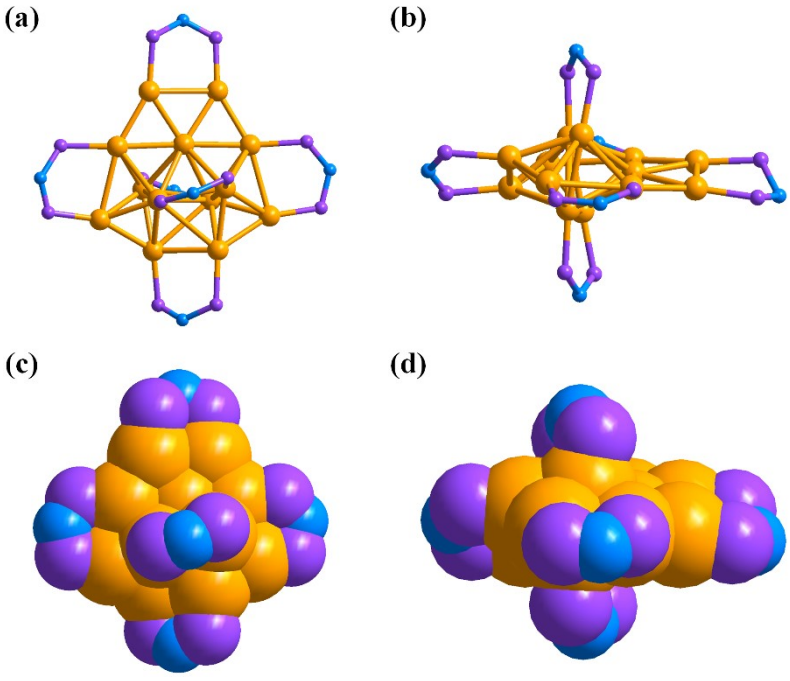

Fig. S5 Molecular structure and space-filling mode of **2**. Color legend: Au, orange; P, purple; N, blue; C, gray. All aromatic rings and hydrogen atoms are omitted for clarity.

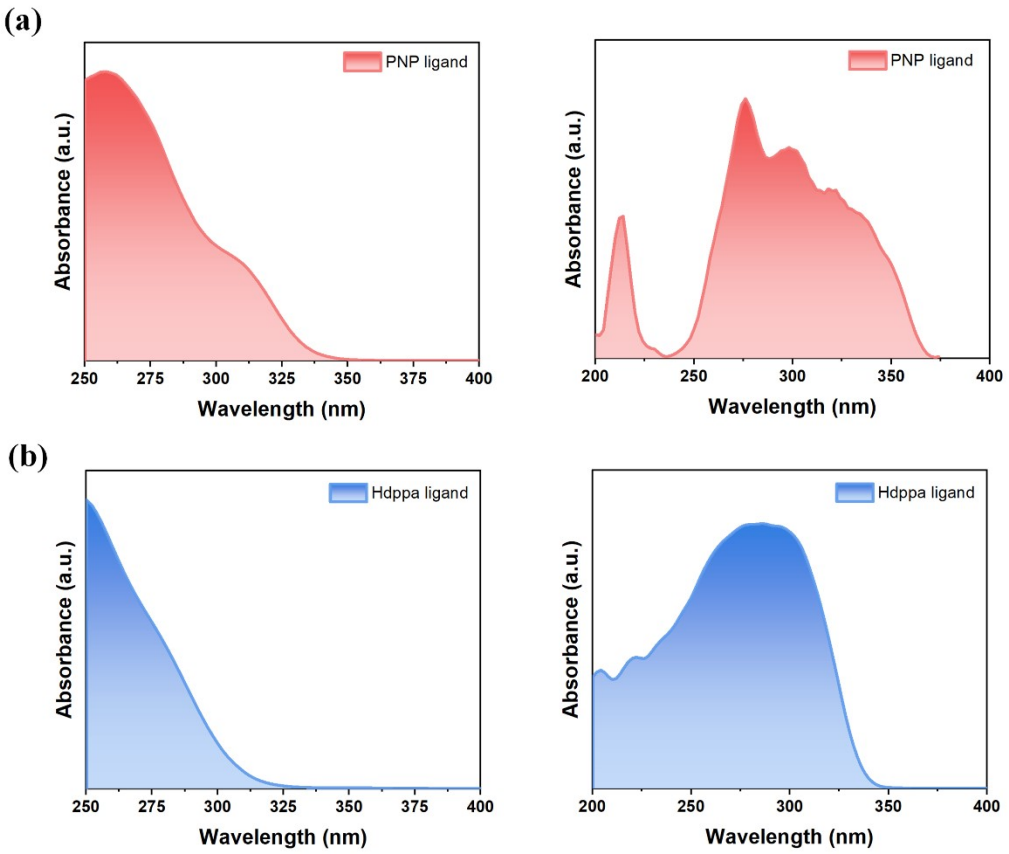

Fig. S6 UV-Vis absorption spectra of PNP (a) and Hdppa (b) ligands in DCM (left) and in solid state (right).

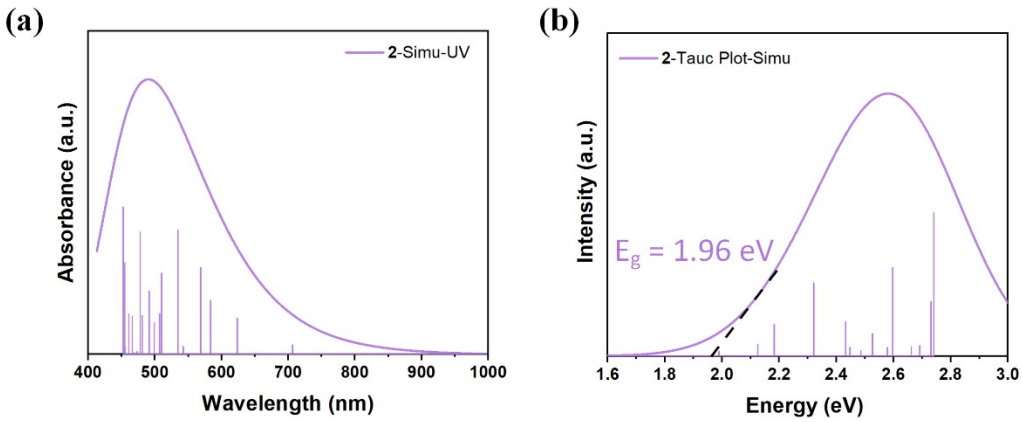

Fig. S7 Calculated TD-DFT UV-Vis absorption spectra (a) and the spectrum on the energy scale (b) of **2**.

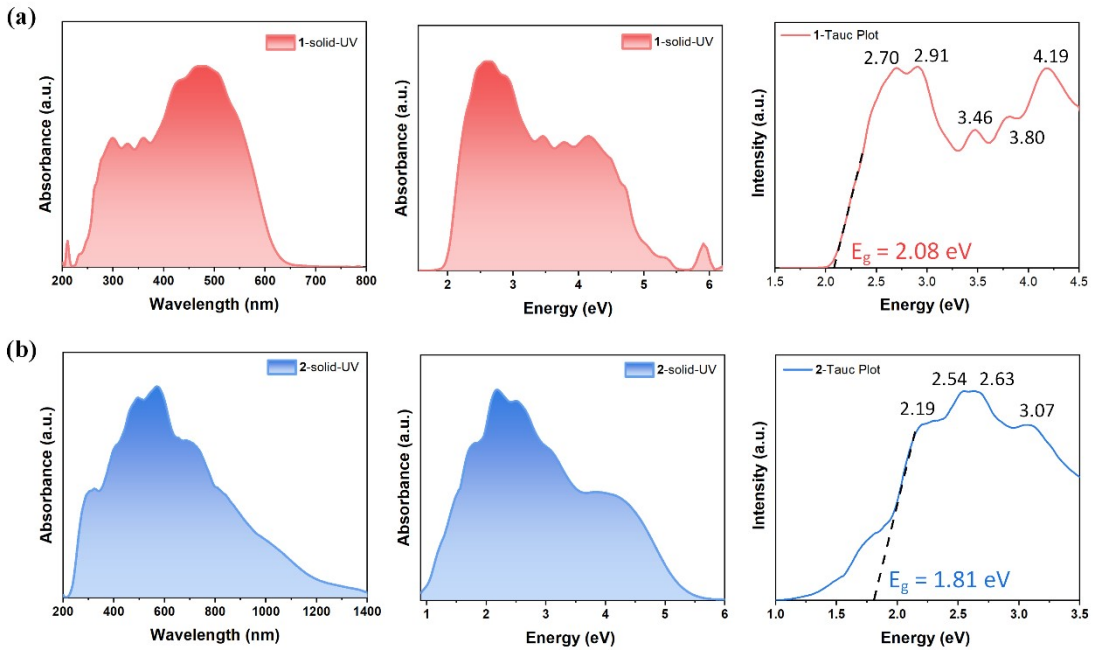

Fig. S8 UV-Vis absorption spectra (left and middle) and them on the energy scale (right) of **1** (a) and **2** (b) in solid state. The optical gaps are determined to be about 2.08 eV (**1**) and 1.81 eV (**2**).

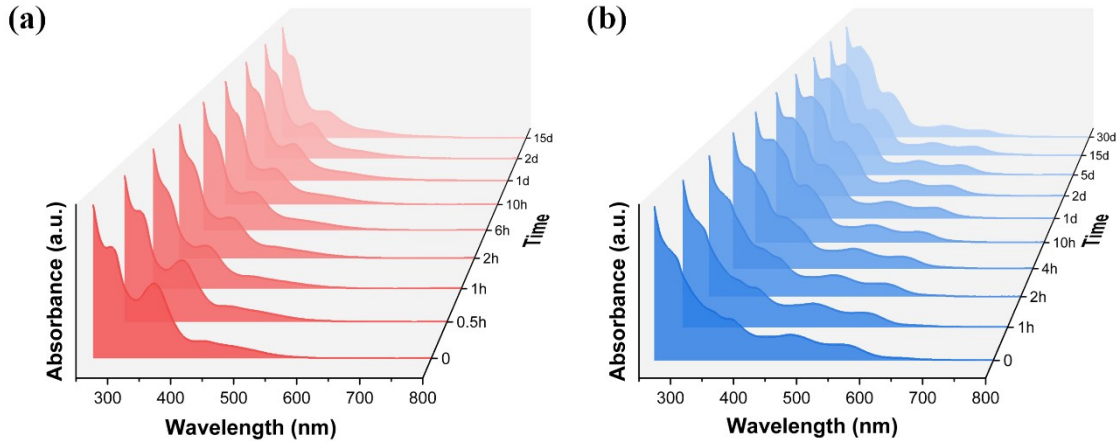

Fig. S9 Time-dependent UV-Vis absorption spectra in DCM of **1** (a) and **2** (b).

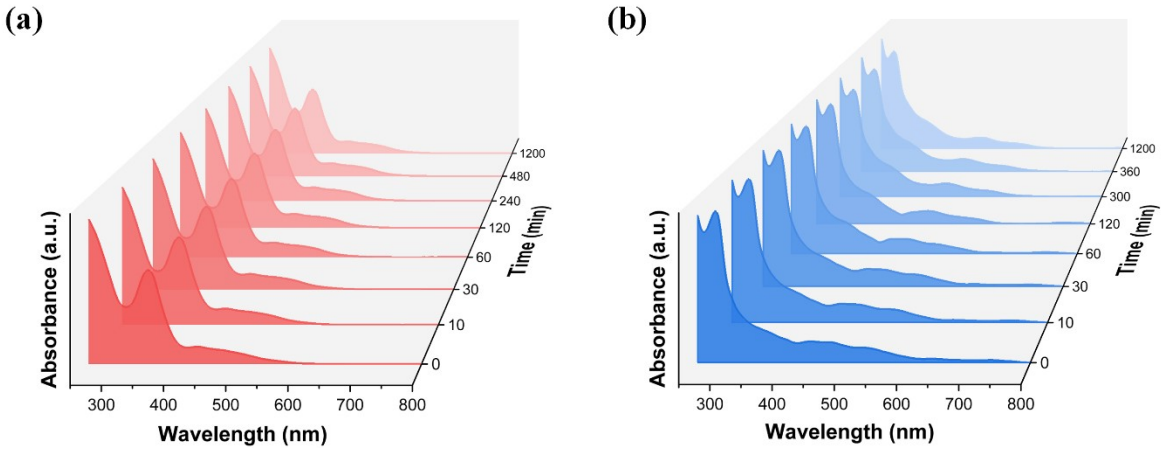

Fig. S10 Time-dependent UV-Vis absorption spectra in 50°C EtOH of **1** (a) and **2** (b).

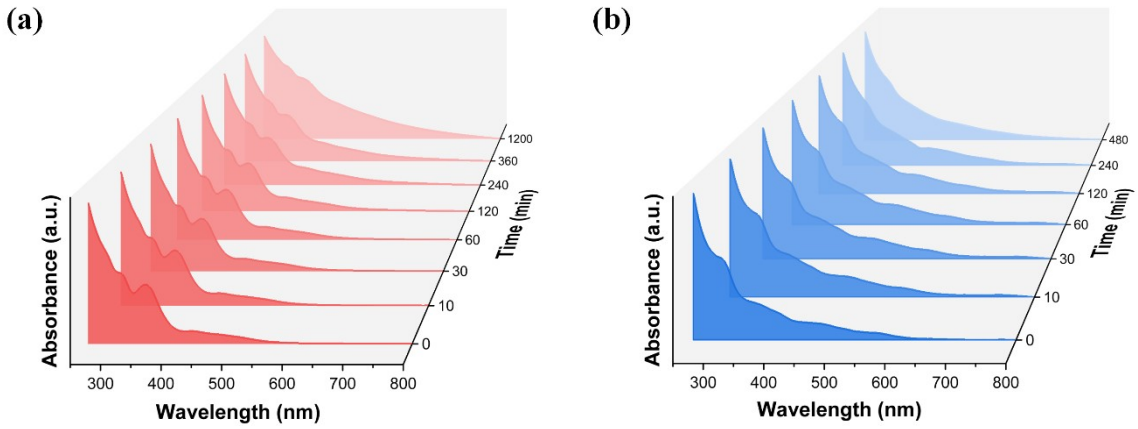

Fig. S11 Time-dependent UV-Vis absorption spectra in EtOH solution containing 0.1 M NaOH of **1** (a) and **2** (b).

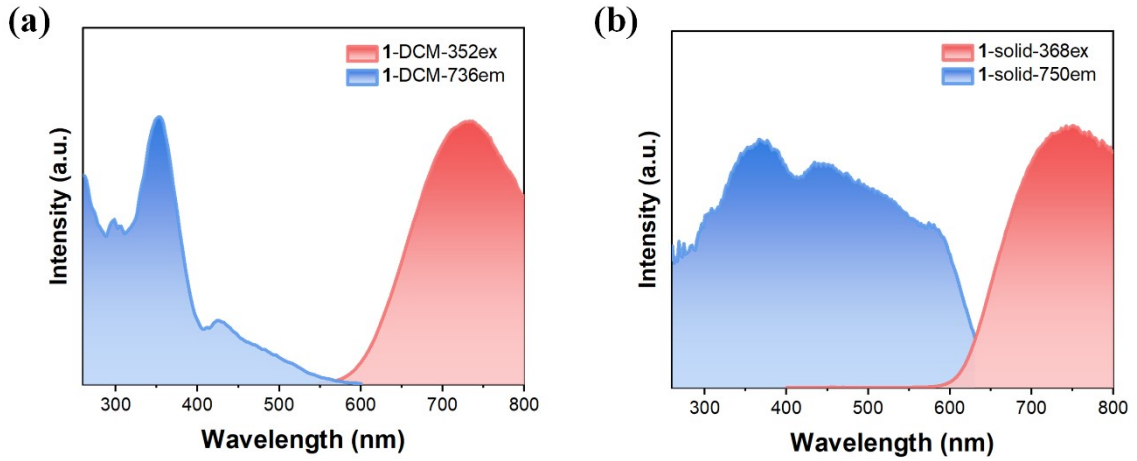

Fig. S12 Fluorescence spectra of **1** in DCM (a) and in solid state (b) at RT.

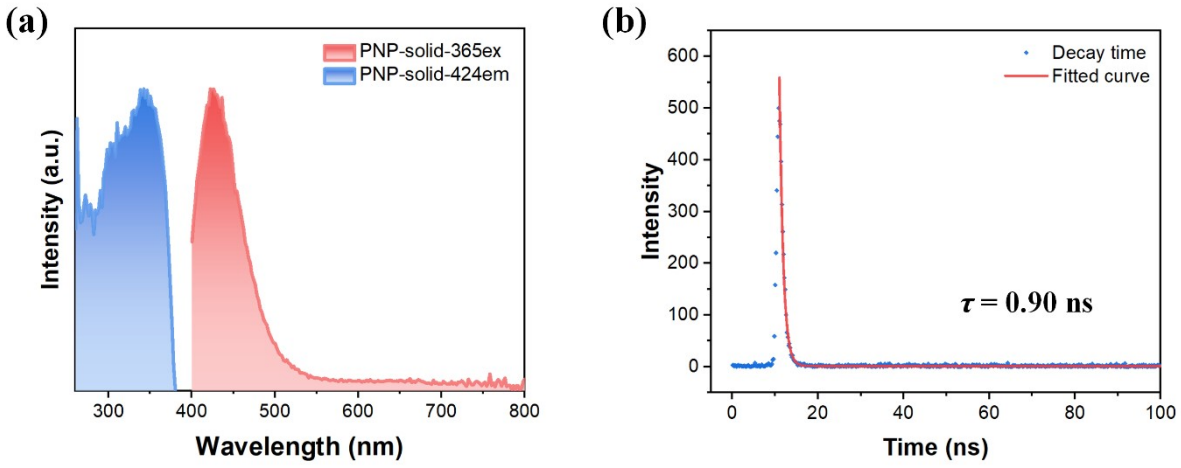

Fig. S13 Fluorescence spectra (a) and luminescence lifetime decay plot (b) of PNP ligand in solid state at RT.

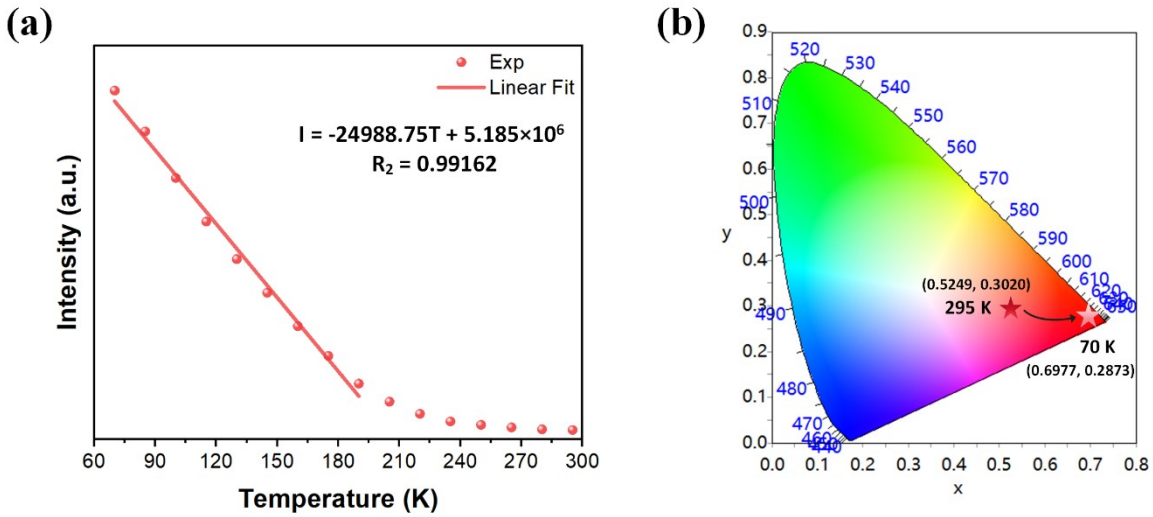

Fig. S14 The correlation between the temperature and emission intensity (a) of NCs **1** and CIE color coordinates (b).

Table S1. Crystal data and structure refinement for **1**.

Empirical formula	$C_{146}H_{119}Au_{13}Cl_5N_5OP_{10}$
Formula weight	5006.97
Temperature / K	150
Crystal system	orthorhombic
Space group	*Pbca*
a / Å	31.9023(4)
b / Å	27.8580(4)
c / Å	34.1479(5)
α / °	90
β / °	90
γ / °	90
Volume / Å^3	30348.4(8)
Z	8
ρ_{calc} (g / cm^3)	2.192
μ / mm^{-1}	25.15
F (000)	18400
Crystal size / mm^3	0.12 × 0.02 × 0.01
Radiation	Cu Kα (λ = 1.54184)
2θ range for data collection / °	5.176 to 124.996
Index ranges	-36 ≤ h ≤ 24, -32 ≤ k ≤ 25, -39 ≤ l ≤ 39
Reflections collected	74245
Independent reflections	24196 [R_{int} = 0.1253, R_{sigma} = 0.1337]
Data/restraints/parameters	24196/1104/1569
Goodness-of-fit on F^2	0.915
Final R indexes [I >= 2σ(I)]	R_1 = 0.0805, wR_2 = 0.1949
Final R indexes [all data]	R_1 = 0.1230, wR_2 = 0.2142
Largest diff. peak/hole / e Å^{-3}	4.35/–4.97
CCDC No.	2330058

[a] $R_1 = \sum||F_o| - |F_c||/\sum|F_o|$. $wR_2 = [\sum w(F_o^2 - F_c^2)^2/\sum w(F_o^2)^2]^{1/2}$.

Table S2. Crystal data and structure refinement for **2**.

Empirical formula	$C_{144}H_{126}Au_{13}Cl_5N_6P_{12}$
Formula weight	5049.96
Temperature / K	210.00
Crystal system	orthorhombic
Space group	$Pna2_1$
a / Å	53.647(5)
b / Å	14.0631(13)
c / Å	20.9828(19)
α / °	90
β / °	90
γ / °	90
Volume / Å^3	15830(3)
Z	4
ρ_{calc} (g / cm^3)	2.119
μ / mm^{-1}	16.649
F (000)	9296
Crystal size / mm^3	0.18 × 0.11 × 0.06
Radiation	Ga Kα (λ = 1.34138)
2θ range for data collection / °	6.738 to 113.998
Index ranges	-66 ≤ h ≤ 67, -17 ≤ k ≤ 16, -24 ≤ l ≤ 26
Reflections collected	250228
Independent reflections	30528 [R_{int} = 0.0613, R_{sigma} = 0.0322]
Data/restraints/parameters	30528/1014/1307
Goodness-of-fit on F^2	1.114
Final R indexes [I >= 2σ(I)]	R_1 = 0.0590, wR_2 = 0.1830
Final R indexes [all data]	R_1 = 0.0776, wR_2 = 0.1949
Largest diff. peak/hole / e Å^{-3}	1.49/-1.12
CCDC No.	2330057

[a] $R_1 = \sum||F_o| - |F_c||/\sum|F_o|$. $wR_2 = [\sum w(F_o^2 - F_c^2)^2/\sum w(F_o^2)^2]^{1/2}$.

Table S3. A summary of Au–Au distances in **1**.

	Au–Au distance / Å	Average value / Å
Au_7^1	2.7323(13)–2.9604(13)	2.855
Au_7^2	2.7648(12)–2.9290(13)	2.842
between Au_7^1 and Au_7^2	2.8623(13)–3.1413(13)	2.991

Table S4. A summary of Au–Cl/P and Au···N distances in **1** and **2**.

	Distance / Å	Average value / Å
Au–Cl (**1**)	2.326(6), 2.338(6)	2.332
Au–P (**1**)	2.281(6)–2.325(6)	2.301
Au–P (**2**)	2.191(8)–2.392(9)	2.308
Au···N (**1**)	2.9896(16)–3.0910(17)	3.029
Au···N (**2**)	3.1740(20)–3.4873(19)	3.364

Table S5. A summary of Au–Au distances in **2**.

	Au–Au distance / Å	Average value / Å
Au_7^1	2.7151(18)–3.3597(14)	2.892
Au_7^2	2.7160(2)–3.3597(14)	2.890
between Au_7^1 and Au_7^2	2.8695(15)–3.3597(14)	3.002
between Au_{11} and Au_2	2.6499(19)–2.7001(16)	2.677
Au_2	3.0106(16)	/

Table S6. P···P distances of disphosphine ligands of selected Au_x NCs ($x \leq 20$).

NCs	P···P distance / Å	Average value / Å	Reference*
$[Au_{13}(PNP)_5Cl_2]^{3+}$ (**1**)	5.084(8)–5.133(8)	5.113	**this work**
$[Au_{13}(Hdppa)_6]^{5+}$ (**2**)	2.815(11)–2.983(10)	2.899	
$Au_4(dppm)_3I_2$	3.004(3)–3.053(5)	3.030	1
$[Au_6(xy\text{-}xantphos)_3]^{2+}$	4.773(3)–4.873(3)	4.836	2
$[Au_6(mPhDP)_4]^{2+}$	5.418(4)–5.455(4)	5.444	3
$[Au_7(dppp)_4]^{3+}$	4.969(7)–5.333(8)	5.157	4
$[Au_8(dppp)_4Cl_2]^{2+}$	4.810(12)–4.998(12)	4.920	5
$[Au_8(dppp)_4]^{2+}$	4.735(4)–5.396(4)	5.066	
$Au_8(dppf)_4$	4.886(4)–5.285(4)	5.171	6
$[Au_8(PNP)_4]^{+}$	5.455(9)–5.562(8)	5.508	7
$[Au_9(dpph)_4]^{3+}$	5.803(22)–5.902(19)	5.853	8
$[Au_9(BINAP)_4]^{3+}$	4.291(11)–4.541(13)	4.437	9
$[Au_{11}(dppp)_5]^{3+}$	4.458(1)–4.840(2)	4.668	10
$[Au_{11}(dppe)_6]^{3+}$	4.223(5)–4.457(6)	4.306	11
$Au_{11}(dppf)_4Cl_2]^{+}$	5.217(2)–5.291(6)	5.260	6
$[Au_{11}(S\text{-}/R\text{-}DIOP)_4Cl_2]^{+}$	5.523(6)–5.422(6)	5.472	12
$Au_{11}(dpephos)_4Cl_2]^{+}$	5.282(4)–5.433(4)	5.366	13
$Au_{11}(xantphos)_4Cl_2]^{+}$	4.857(5)–4.915(6)	4.886	
$[Au_{11}(dppp)_5]^{+}$	4.454(5)–4.988(5)	4.673	14
$[Au_{11}(PNHP)_4Br_2]^{+}$	5.473(4)–5.822(3)	5.648	
$[Au_{11}(PNCO4\text{-}ClPhP)_4Br_2]^{+}$	5.934(5)–6.054(5)	5.989	
$[Au_{11}(PNCO4\text{-}CO2MePhP)_4Br_2]^{+}$	5.886(13)–6.071(11)	5.984	
$[Au_{11}(PNCO2\text{-}NapP)_4Br_2]^{+}$	5.884(18)–5.977(17)	5.935	
$[Au_{11}(PNCO4\text{-}FPhP)_4Br_2]^{+}$	5.932(8)–6.498(6)	6.101	
$[Au_{13}(dppe)_5Cl_2](PF_6)_3$	4.047(11)–4.122(10)	4.085	15
$[Au_{13}(dppm)_6](BPh_4)_3$	3.068(25)–3.120(24)	3.101	16

$[Au_{13}(dppm)_6]^{5+}$	3.115(3)–3.115(4)	3.115	17
$[Au_{13}[(R)\text{-}L]_5Cl_2]^{3+}$	4.055(23)–4.103(9)	4.090	18
$[Au_{13}(dppe)_5Cl_2]Cl_3$	3.638(18)–4.041(18)	3.810	19
$[Au_{13}(DIPAMP)_5Cl_2]^{3+}$	4.062(21)–4.130(13)	4.096	20
$[Au_{14}(dppp)_5I_4]^{2+}$	4.603(8)–5.588(8)	5.072	21
$[Au_{18}(dppm)_6Cl_4]^{4+}$	3.049(9)–3.129(11)	3.090	22
$[Au_{18}(dppm)_6Br_4]^{2+}$	3.014(4)–3.108(4)	3.073	16
$[Au_{20}(dppm)_6(CN)_6]$	3.036(5)–3.091(5)	3.056	

Table S7. Luminescence lifetime of icosahedral Au_{13}/MAu_{12} NCs in recent publications.

NCs	Temperature	Lifetime (τ) / μs	Reference*
$[Au_{13}(PNP)_5Cl_2]Cl_3$ (**1**)	70 K	**11.63 (τ_{av})**	**this work**
	RT	**6.34 (τ_{av})**	
$[Au_{13}(dppe)_5Cl_2](PF_6)_3$	/	2.69	23
$[Au_{13}(dppe)_5(C{\equiv}CPh)_2](PF_6)_3$		3.51	
$[Au_{13}(NHC\text{-}2)_5Br_2]^{3+}$	RT	2.4	24
$[Au_{13}(NHC\text{-}3)_9Cl_3]^{2+}$		1.2	
$[Au_{13}(bis\text{-}NHC^{Me})_5Br_2]^{3+}$	/	1.03	25
$[Au_{13}(bis\text{-}NHC^{Et})_5Br_2]^{3+}$		0.85	
$[Au_{13}(bis\text{-}NHC^{Bn})_5Br_2]^{3+}$		0.80	
$[Au_{13}(bis\text{-}NHCPyr)_5Cl_2]^{3+}$	/	3.4	26
R-$[Au_{13}(NHC\text{^}MeBz\text{^}Pi)_8Br_4]^{+}$	80 K	3.35	27
	RT	2.53	
$[Au_{13}((S,S)\text{-}DIPAMP)_5Cl_2]^{3+}$	/	3.19	28
$[Au_{13}(PPh_3)_5(2\text{-}S\text{-}QL)_3(2\text{-}SH\text{-}QL)_4]^{2+}$	/	1.58	29
Single-atom-doped Au_{13} (MAu_{12})			
$[RuAu_{12}(dppm)_6]^{2+}$	/	5.7	30
	80 K	24.4	
$[IrAu_{12}(dppm)_6]^{3+}$	RT	6.03	31
$[RhAu_{12}(dppm)_6]^{3+}$		6.96	
$[PtAu_{12}(dppm)_6]^{3+}$		5.71	
$[PdAu_{12}(dppm)_6]^{3+}$		3.07	
$[IrAu_{12}((S,S)\text{-}DIPAMP)_5Cl_2]^{+}$	/	5.87	28

*Reference

1. J. Velden, J. Bour, R. Pet, W. Bosman and J. Noordik, Preparation and X-ray Structure Determination of Tris[bis(diphenylphosphino)methane]diiodotetragold. *Inorg. Chem.*, 1983, **22**, 3112–3115.
2. H. Ito, T. Saito, T. Miyahara, C. Zhong and M. Sawamura, Gold(I) Hydride Intermediate in Catalysis: Dehydrogenative Alcohol Silylation Catalyzed by Gold(I) Complex, *Organometallics*, 2009, **28**, 4829–4840.
3. M. A. Bakar, M. Sugiuchi, M. Iwasaki, Y. Shichibu and K. Konishi, Hydrogen bonds to Au atoms in coordinated gold clusters, *Nat. Commun.*, 2017, **8**, 576.
4. Y. Shichibu, M. Zhang, Y. Kamei and K. Konishi, $[Au_7]^{3+}$: A Missing Link in the Four-Electron Gold Cluster Family, *J. Am. Chem. Soc.*, 2014, **136**, 12892–12895.
5. Y. Kamei, Y. Shichibu and K. Konishi, Generation of Small Gold Clusters with Unique Geometries through Cluster-to-Cluster Transformations: Octanuclear Clusters with Edge-sharing Gold Tetrahedron Motifs, *Angew. Chem. Int. Ed.*, 2011, **50**, 7442–7445.
6. L.-Y. Yao and V. W.-W. Yam, Diphosphine-Stabilized Small Gold Nanoclusters: From Crystal Structure Determination to Ligation-Driven Symmetry Breaking and Anion Exchange Properties, *J. Am. Chem. Soc.*, 2016, **138**, 15736–15742.
7. T.-S. Zhang, W. Fei, N. Li, Y. Zhang, C. Xu, Q. Luo and M.-B. Li, Open Nitrogen Site-Induced Kinetic Resolution and Catalysis of a Gold Nanocluster, *Nano Lett.*, 2022, **23**, 235–242.
8. M. Schulz-Dobrick and M. Jansen, Characterization of Gold Clusters by Crystallization with Polyoxometalates: the Intercluster Compounds $[Au_9(dpph)_4][Mo_8O_{26}]$, $[Au_9(dpph)_4][PW_{12}O_{40}]$ and $[Au_{11}(PPh_3)_8Cl_2]_2[W_6O_{19}]$, *Z. Anorg. Allg. Chem.*, 2007, **633**, 2326–2331.
9. J.-Q. Wang, Z.-J. Guan, W.-D. Liu, Y. Yang and Q.-M. Wang, Chiroptical Activity Enhancement via Structural Control: The Chiral Synthesis and Reversible Interconversion of Two Intrinsically Chiral Gold Nanoclusters, *J. Am. Chem. Soc.*, 2019, **141**, 2384–2390.

10. J. Smits, J. Bour, F. Vollenbroek and P. Beurskens, Preparation and X-ray structure determination of [pentakis{1,3-bis(diphenylphosphino)propane}] undecagoldtris(thiocyanate), $[Au_{11}\{PPh_2C_3H_6PPh_2\}_5](SCN)_3$. *J. Crystallogr. Spectrosc. Res.*, 1983, **13**, 355.
11. Y. Shichibu, Y. Kamei and K. Konishi, Unique [core+two] structure and optical property of a dodeca-ligated undecagold cluster: critical contribution of the exo gold atoms to the electronic structure, *Chem. Commun.*, 2012, **48**, 7559–7561.
12. S. Takano and T. Tsukuda, Amplification of the Optical Activity of Gold Clusters by the Proximity of BINAP, *J. Phys. Chem. Lett.*, 2016, **7**, 4509–4513.
13. T.-H. Huang, F.-Z. Zhao, Q.-L. Hu, Q. Liu, T.-C. Wu, D. Zheng, T. Kang, L.-C. Gui and J. Chen, Bisphosphine-Stabilized Gold Nanoclusters with the Crown/Birdcage-Shaped Au11 Cores: Structures and Optical Properties, *Inorg. Chem.*, 2020, **59**, 16027–16034.
14. Y. Zhang, S.-R. He, Y. Yang, T.-S. Zhang, Z.-M. Zhu, W. Fei and M.-B. Li, Preorganized Nitrogen Sites for Au_{11} Amidation: A Generalizable Strategy toward Precision Functionalization of Metal Nanoclusters, *J. Am. Chem. Soc.*, 2023, **145**, 12164–12172.
15. Y. Shichibu and K. Konishi, HCl-induced nuclearity convergence in diphosphine-protected ultrasmall gold clusters: a novel synthetic route to "magic-number" Au_{13} clusters, *Small*, 2010, **6**, 1216–1220.
16. S. Jin, W. Du, S. Wang, X. Kang, M. Chen, D. Hu, S. Chen, X. Zou, G. Sun and M. Zhu, Thiol-Induced Synthesis of Phosphine-Protected Gold Nanoclusters with Atomic Precision and Controlling the Structure by Ligand/Metal Engineering, *Inorg. Chem.*, 2017, **56**, 11151–11159.
17. S.-S. Zhang, L. Feng, R. D. Senanayake, C. M. Aikens, X.-P. Wang, Q.-Q. Zhao, C.-H. Tung and D. Sun, Diphosphine-protected ultrasmall gold nanoclusters: opened icosahedral Au_{13} and heart-shaped Au_8 clusters, *Chem. Sci.*, 2018, **9**, 1251–1258.
18. Y. Yang, Q. Zhang, Z.-J. Guan, Z.-A. Nan, J.-Q. Wang, T. Jia and W.-W. Zhan, Enantioselective Synthesis of Homochiral Au_{13} Nanoclusters and Their Chiroptical Activities, *Inorg. Chem.*, 2019, **58**, 3670–3675.
19. J. Zhang, Y. Zhou, K. Zheng, H. Abroshan, D. R. Kauffman, J. Sun and G. Li, Diphosphine-induced chiral propeller arrangement of gold nanoclusters for singlet oxygen photogeneration, *Nano Res.*, 2018, **11**, 5787–5798.
20. Y. Shichibu, Y. Ogawa, M. Sugiuchi and K. Konishi, Chiroptical activity of Au_{13} clusters: experimental and theoretical understanding of the origin of helical charge movements, *Nanoscale Adv.*, 2021, **3**, 1005–1011.
21. H. Zhao, Q. You, W. Zhu, J. Li, H. Deng, M. B. Li, Y. Zhao and Z. Wu, Nanoclusterzyme for Dual Colorimetric Sensings: A Case Study on $[Au_{14}(Dppp)_5I_4]^{2+}$, *Small*, 2023, **19**, 2207936.
22. S.-S. Zhang, R. D. Senanayake, Q.-Q. Zhao, H.-F. Su, C. M. Aikens, X.-P. Wang, C.-H. Tung, D. Sun and L.-S. Zheng, $[Au_{18}(dppm)_6Cl_4]^{4+}$: a phosphine-protected gold nanocluster with rich charge states, *Dalton Trans.*, 2019, **48**, 3635–3640.
23. M. Sugiuchi, Y. Shichibu, T. Nakanishi, Y. Hasegawa and K. Konishi, Cluster-π Electronic Interaction in A Superatomic Au_{13} Cluster Bearing Sigma-Bonded Acetylide Ligands. *Chem. Commun.*, 2015, **51**, 13519–13522.
24. H. Shen, S. Xiang, Z. Xu, C. Liu, X. Li, C. Sun, S. Lin, B. K. Teo and N. Zheng, Superatomic Au_{13} Clusters Ligated by Different N-Heterocyclic Carbenes and Their Ligand-Dependent Catalysis, Photoluminescence, and Proton Sensitivity. *Nano Res.*, 2020, **13**, 1908–1911.
25. P. Luo, S. Bai, X. Wang, J. Zhao, Z. N. Yan, Y. F. Han, S. Q. Zang and T. C. W. Mak, Tuning the Magic Sizes and Optical Properties of Atomically Precise Bidentate N-Heterocyclic Carbene-Protected Gold Nanoclusters via Subtle Change of N-Substituents. *Adv. Optical Mater.*, 2021, **9**, 2001936.
26. X. Wang, R. Liu, L. Tian, J. Bao, C. Zhao, F. Niu, D. Cheng, Z. Lu and K. Hu, Highly Luminescent NHC-Stabilized Au_{13} Clusters as Efficient Excited-State Electron Donors. *J. Phys. Chem. C*, 2022, **126**, 18374–18382.
27. P. Luo, X. J. Zhai, S. Bai, Y. B. Si, X. Y. Dong, Y. F. Han and S. Q. Zang, Highly Efficient Circularly Polarized Luminescence from Chiral Au_{13} Clusters Stabilized by Enantiopure Monodentate NHC Ligands. *Angew. Chem. Int. Ed.*, 2023, **62**, e202219017.
28. H. Hirai, T. Nakashima, S. Takano, Y. Shichibu, K. Konishi, T. Kawai and T. Tsukuda, $IrAu_{12}$ Superatom Modified by Chiral Diphosphines: Doping-Induced Enhancement of Chiroptical Activity. *J. Mater. Chem. C*, 2023, **11**, 3095–3100.
29. X.-J. Zhai, J.-H. Hu, J. Guan, Y. Si, X.-Y. Dong, P. Luo, F. Pan, Z. Yu, R. Han and S.-Q. Zang, Luminescence Modulation of Ultrasmall Gold Clusters by Aromatic Ligands. *Nano Res.*, 2023, **16**, 11366–11374.
30. S. Takano, H. Hirai, T. Nakashima, T. Iwasa, T. Taketsugu and T. Tsukuda, Photoluminescence of Doped Superatoms $M@Au_{12}$ (M = Ru, Rh, Ir) Homoleptically Capped by $(Ph_2)PCH_2P(Ph_2)$: Efficient Room-Temperature Phosphorescence from $Ru@Au_{12}$. *J. Am. Chem. Soc.*, 2021, **143**, 10560−10564.
31. H. Hirai, S. Takano, T. Nakashima, T. Iwasa, T. Taketsugu and T. Tsukuda, Doping-Mediated Energy-Level Engineering of $M@Au_{12}$ Superatoms (M=Pd, Pt, Rh, Ir) for Efficient Photoluminescence and Photocatalysis. *Angew. Chem. Int. Ed.*, 2022, **61**, e202207290.